Modern Grid Strategy:

Enhanced GridLAB-D Capabilities Final Report

October 9th 2009

Kevin P. Schneider Ph.D., P.E.
Jason Fuller
Frank Tuffner Ph.D.
Yousu Chen

Pacific Northwest
NATIONAL LABORATORY

Table of Contents

1. Introduction

GridLAB-D is a software simulation environment that was initially developed by the United States Department of Energy (DOE) Office of Electricity (OE) for the purpose of enabling the effective analysis of the emerging smart grid technologies. In order to achieve this goal, GridLAB-D was developed using an open source approach with the intent that numerous people and organizations would contribute to the ongoing development. Because of the breadth and complexity of the emerging smart grid technologies, the inclusion of multiple groups of developers is essential in order to address the many aspects of the smart grid.

As part of the continuing Modern Grid Strategy (MGS), the Pacific Northwest National Laboratory (PNNL) has been tasked with developing an advanced set of GridLAB-D capabilities. These capabilities were developed to enable the analysis of complex use case studies which will allow for multi-disciplinary analysis of smart grid operations. The advanced capabilities which were developed include the implementation of an unbalanced networked power flow algorithm, the implementation of an integrated transmission and distribution system solver, and a set of use cases demonstrating the capabilities of the new solvers. The following sections contained detailed descriptions of the enhanced capabilities; the relevant source code may be obtained at [1].

2. Power Flow

This section explains the technical aspects of the distribution power flow implemented in GridLAB-D. The power flow module provides electrical distribution system modeling for power flow solutions. A power flow calculation is performed to determine the steady state node voltages and line currents at each point in the given model system, electrical loads connected at each node, and voltage at the substation. In the initial release, GridLAB-D implemented the well established Forward Backward Sweep (FBS) algorithm [2]. While this is an efficient and robust algorithm, it does not readily permit for the analysis of systems that are meshed. This limits the analysis to radial distribution systems; transmission systems, sub-transmission, and meshed distribution feeders were not supported. To address this issue, a networked solver was integrated into GridLAB-D.

The first attempt at integrating a networked solver used a Gauss Seidel (GS) implementation which did not prove successful. The network solver that was successfully implemented was based on a Newton Raphson (NR) implementation. The following subsections discuss the three algorithms, FSB, GS, and NR, including their strengths and weaknesses, as well as their appropriateness for use.

2.1 Forward Backward Sweep

The FBS solution method was one of the first effective solvers for unbalanced radial distribution systems. It is an efficient and robust algorithm, but it has the severe limitation of only being able to solve radial topologies. Despite this limitation, well over 95% of the distribution feeders in North America are topologically radial, and as a result, the FBS algorithm is widely used.

The FBS method is a two step process [2]. In the first step, the currents at each node are summed. Then using Kirchhoff's Current Law, the currents are summed node by node until the current being supplied by the substation is determined. This current, along with line values and load parameters, is used to determine the voltage drop across each line section in the distribution feeder. A complete sweep, first backward and then forward, constitutes a single power flow iteration. Equation (2.1) shows the current summation for a single node while (2.2) shows the voltage drop calculation across a single link.

backward sweep

$$[I_{abc}]_n = [c] \cdot [V_{abc}]_m + [d] \cdot [I_{abc}]_m \qquad (2.1)$$

forward sweep

$$[V_{abc}]_m = [A] \cdot [V_{abc}]_n - [B] \cdot [I_{abc}]_m \qquad (2.2)$$

where the *c, d, A,* and *B* matrices represent individual characteristics of each link section as described in Kersting [2].

2.2 Gauss Seidel Method

The Gauss Seidel algorithm was one of the first algorithms implemented for balanced transmission power flow solvers, but it had never been applied to distribution system analysis. The generalized formulation of the Gauss Seidel algorithm is shown in (2.3-2.6) [3].

General Node Injection Formula:

$$S_m^j = V_m^j \cdot \sum_{k=1}^{n} \left[\sum_{t \in p} \left[(y_{jt})_{mk}^* \cdot (V_k^t)^* \right] \right] \qquad (2.3)$$

where:

> j = phase a, b, or c,
> m = bus number,
> n = number of buses, and
> $p = \{a, b, c\}$.

For Swing buses: Voltage and angle are constant.

For PQ buses:

$$V_m^j = \frac{1}{\left(y_{jj}\right)_{mm}}\left[\left(\frac{P_m^j + Q_m^j}{V_m^j}\right)^* - \sum_{\substack{k=1 \\ k \neq m}}^{n}\left[\sum_{t \in p}\left[\left(y_{jt}\right)_{mk}^* \cdot \left(V_k^t\right)^*\right] - \sum_{\substack{t \in p \\ t \neq j}}\left[\left(y_{jt}\right)_{mk}^* \cdot \left(V_k^t\right)^*\right]\right]\right] \tag{2.4}$$

For PV buses:

$$V_m^j = \frac{1}{\left(y_{jj}\right)_{mm}}\left[\left(\frac{P_m^j + Q_m^j}{V_m^j}\right)^* - \sum_{\substack{k=1 \\ k \neq m}}^{n}\left[\sum_{t \in p}\left[\left(y_{jt}\right)_{mk}^* \cdot \left(V_k^t\right)^*\right] - \sum_{\substack{t \in p \\ t \neq j}}\left[\left(y_{jt}\right)_{mk}^* \cdot \left(V_k^t\right)^*\right]\right]\right] \tag{2.5}$$

$$Q_m^j = \text{Im}\left[V_m^j \cdot \sum_{k=1}^{n}\left[\sum_{t \in p}\left[\left(y_{jt}\right)_{mk}^* \cdot \left(V_k^t\right)^*\right]\right]\right] \tag{2.6}$$

One of the reasons that the Gauss Seidel method was initially investigated was the potential for utilizing High Performance Computing (HPC) assets. From (2.3-2.6), it can be seen that the calculations at any given node are independent from other nodes in the system. In theory it is possible for multiple processors to operate on a single problem, assuming that memory access was properly handled.

Once the Gauss Seidel algorithm was implemented, it was quickly determined that it would not be a viable method for large distribution systems. Because of the need for error corrections to propagate through the system, the computational requirements, even for medium sized models, were prohibitive. Even the potential for utilizing HPC resources was not sufficient to offset the computational requirements. An example of this can be seen by the time that is required to solve the IEEE 34 node test feeder. A complete solution to this system requires <1 second for the FBS algorithm, while the Gauss Seidel algorithm takes >10 minutes. If this is scaled to a full size system, such as one of the prototypical feeders developed in FY09, use of the Gauss Seidel algorithm was quickly shown to be infeasible as implemented.

3

2.3 Newton Raphson Method

The Newton Raphson algorithm has also found wide spread use in transmission analysis, but it has also been shown an effective algorithm for distribution system analysis [4]. The Newton-Raphson solver is comprised of two principle sets of equations. The first set of equations describes the current injection from loads into the system. They are split into a real and imaginary component and are given as:

$$\Delta I_{rk}^s = \frac{\left(P_k^{sp}\right)^s V_{rk}^s + \left(Q_k^{sp}\right)^s V_{mk}^s}{\left(V_{rk}^s\right)^s + \left(V_{mk}^s\right)^s} - \sum_{i=1}^{n}\sum_{t}\left(G_{ki}^{st}V_{ri}^{st} - B_{ki}^{st}V_{mi}^t\right) \tag{2.7}$$

$$\Delta I_{mk}^s = \frac{\left(P_k^{sp}\right)^s V_{mk}^s + \left(Q_k^{sp}\right)^s V_{rk}^s}{\left(V_{rk}^s\right)^s + \left(V_{mk}^s\right)^s} - \sum_{i=1}^{n}\sum_{t}\left(G_{ki}^{st}V_{mi}^{st} - B_{ki}^{st}V_{ri}^t\right) \tag{2.8}$$

where:

ΔI_{rk} is the real current injection at the bus,

ΔI_{mk} is the imaginary current injection at the bus,

k is the bus number,
s is the current phase of interest $\{a,b,c\}$,
t represents all the phases connected to the bus,
P_k is the real power component of the load at bus k, and
Q_k is the imaginary power component of the load at bus k.

With the current injections calculated, the voltage updates are computed via:

$$\begin{bmatrix} \Delta I_{mk} \\ \Delta I_{rk} \end{bmatrix} = -J^{-1}\begin{bmatrix} \Delta V_{rk} \\ \Delta V_{mk} \end{bmatrix} \tag{2.9}$$

where J^{-1} represents the inverse Jacobian given by $J = \begin{bmatrix} \dfrac{\delta\Delta I_{mk}}{\delta\Delta V_{rk}} & \dfrac{\delta\Delta I_{mk}}{\delta\Delta V_{mk}} \\ \dfrac{\delta\Delta I_{rk}}{\delta\Delta V_{rk}} & \dfrac{\delta\Delta I_{rk}}{\delta\Delta V_{mk}} \end{bmatrix}$.

As with the Gauss-Seidel method, one node must be designated a swing or slack bus. This node will represent an infinite bus and provides the fixed voltage reference for the solver iterations.

3. Transmission and Distribution Integration

One of the key issues surrounding the analysis of smart grid technologies is how to maximize the value of the deployed assets. Only assessing the local benefits of such assets may undervalue their overall impact on the system. For example, while a shunt capacitor may be installed to provide a more optimal voltage profile on a distribution feeder, it is also reducing the reactive power requirements of generators on the transmission system. Also, large penetrations of renewable resources on the distribution system will have an impact on the operations of the transmission system.

Since transmission and distribution system analysis have been treated as two separate systems, it has been difficult to examine their interactions. For this reason, the MGS decided to add an integrated solver to GridLAB-D which would allow for the transmission and distribution systems to be combined into a single, unified model. The difficulty in creating a unified model is that distribution system models are full per-phase unbalanced models, while transmission models assume a three-phase balanced system. Because of the large number of distribution feeders, the assumption of a balanced transmission system is often valid. For distribution systems, unbalances of 10%-15% are not uncommon. In the presence of a large number of distribution feeders, the numerous unbalances will average out and appear balanced from the transmission system perspective. If there are a relatively small number of heavily unbalanced distribution feeders, then the assumption of a balanced transmission system is not longer valid. Since there were limited examples of how to address this issue, two approaches were initially considered: a boundary condition method and an integrated method.

3.1 Boundary Condition Method

The first potential solution that was considered was to treat the transmission and distribution systems as two separate parts of the model and to match the boundary values. In this case, the boundary values are the distribution side voltage and the transmission side currents. The distribution voltages would be "inherited" from the transmission system, and the distribution currents would be balanced and passed to the transmission system. In this situation, the distribution system would use the per-phase unbalanced solution methods, and the transmission system would use the traditional balanced power flow algorithms.

From this description, it is clear that there are a number of assumptions that would introduce potential error into the simulation results. The most significant of these is how the unbalanced load of the distribution system is balanced and applied to the transmission system. Because of the loss of detail associated with such a simplification, it was decided that a boundary condition method was not appropriate for implementation in GridLAB-D.

3.2 Integrated Method

In the integrated method both the transmission and distribution systems are modeled as per-phase unbalanced systems. When the systems are modeled in this way, there are no simplifications, and as a result, it is a more accurate representation of the physical infrastructure. One issue that had to be addressed was that of transmission line transposition [3]. In order to facilitate analytic studies of

transmission system operations, the transmission lines have been historically transposed during construction. As a result of this, it is necessary for transmission line segments in GridLAB-D to be divided into three separate segments, each with a different phase configuration. Once the proper transmission line models are implemented, the transmission and distribution systems are connected via transformers at the substation. In general, these are Delta-Wye step-down transformers, but other types can be used if desired.

Note: Since the integrated method involves a networked transmission system, it is necessary to use the Newton Raphson solver; the FBS algorithm will not solve properly.

4. Selected Use Case Scenarios

This section will discuss four (4) use cases that were developed to highlight the utility of the algorithms that were implemented in the previous sections. These use cases will focus on using the Newton Raphson solver to investigate how events on the distribution system affect the operation of the transmission system. These use cases are meant to highlight the capabilities of the new algorithms. They are not meant as complete analyses.

4.1 Use Case System Model

The use case system models consist of a six node, networked sub-transmission system and ten radial feeders with 633 primary nodes each, connected at various points through Delta-Wye transformers, as seen in Figure 4.1. The total system solved, once secondary nodes are considered, has nearly 22,000 one-, two-, and three-phase nodes, and over 50,000 independently controlled objects. The networked transmission system operates at 138 kV and consists of 5-15 mile lines using a three-phase delta-connected system. Even though the transmission system does not have a neutral conductor, one was included to model the capacitance from the phase conductors to the earth ground. The included neutral conductor was not connected to the delta connected transmission system; it was simply in parallel approximating an earth ground. The phase conductors are Aluminum Cable Steel Reinforced (ACSR) 447 kcmil Hen type with an ampacity rating of 666 Amps. Figure 4.2 shows the arrangement of the phase conductors.
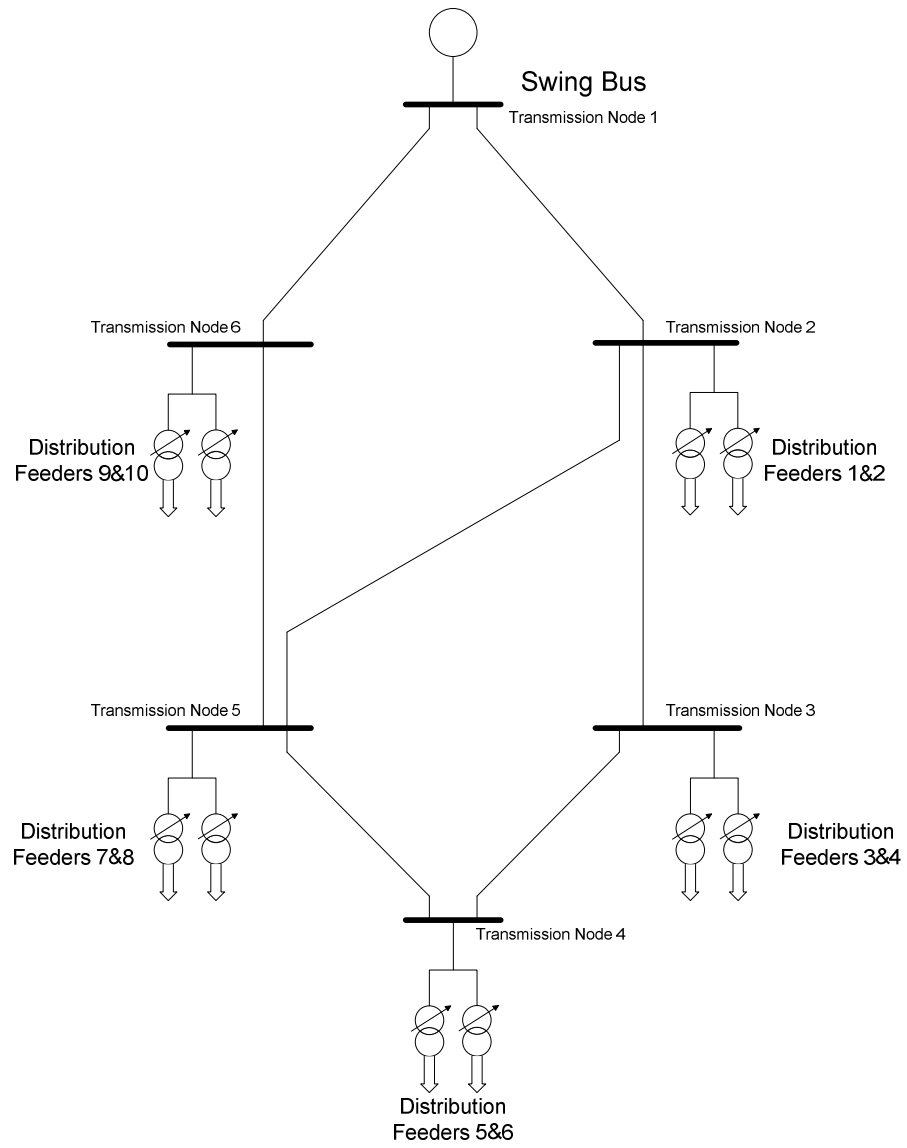
**Figure 4.1: Distribution feeders and interconnecting sub-transmission system**
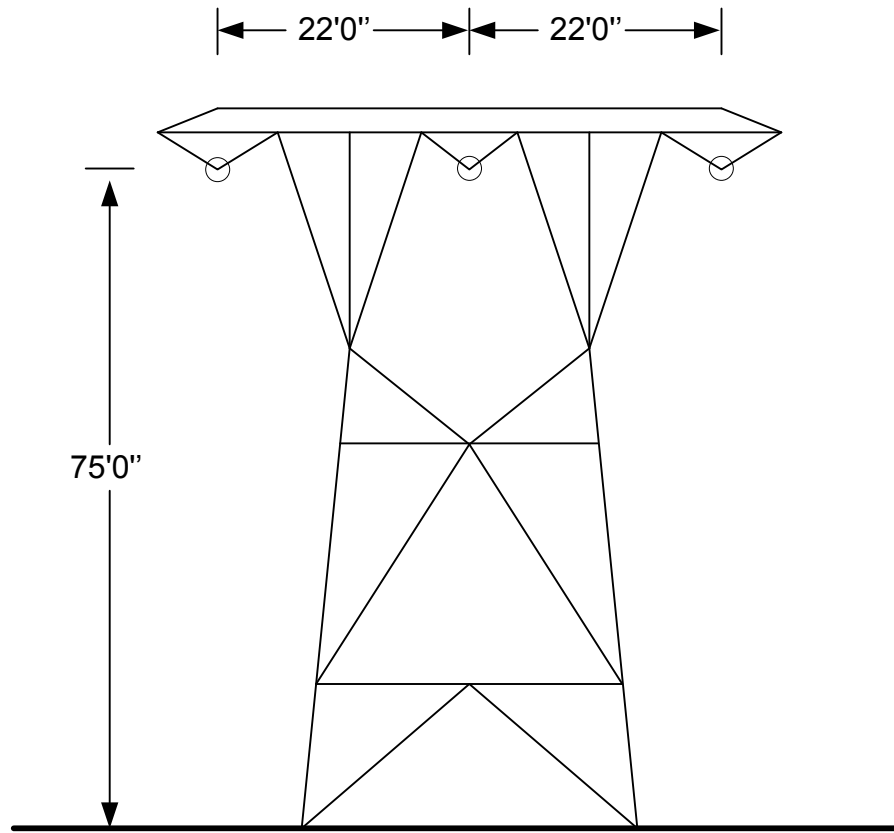
Figure 4.2: Transmission conductor configuration

The ten distribution feeders were built by modifying the R3-12.47-1 taxonomy feeder [5]. The R3-12.47-1 feeder is representative of a heavily populated urban area in the southwestern region of the United States. It is composed of single family homes, heavy commercial loads, and a small amount of light industrial loads. Approximately 25% of the circuit-feet are overhead and 75% underground. The majority of the load is located relatively near the substation. Table 4.1 shows the general information about the generic R3-12.47-1 taxonomy feeder.

Table 4.1: Taxonomy Feeder R3-12.47-1 original configuration

Nodes	633
Voltage (kV)	12.47
Load (kW)	8,400
Voltage Regulators	0
Reclosers	0
Residential Transformers	383
Commercial Transformers	58
Industrial Transformers	0
Agricultural Transformers	0

From Table 4.1, it can be seen that the maximum load on the feeder is 8,400 kW. In order to properly represent the system during time-series simulations, it is necessary to model the individual loads. In the system model, the static residential transformer loads are replaced with 50% time-varying constant power loads and 50% thermodynamic residential house models, totaling nearly 2200 thermodynamic residential models. The residential models also include additional detailed end-use loads such as lights, plug loads, HVAC systems, and water heaters. Static commercial and industrial loads are replaced with historical time-varying loads. The base case generation and loading is shown in Figure 4.3. In the base case, all of the generation is supplied by the swing bus and the difference between the two lines in Figure 4.3 represents the losses in the transmission system.
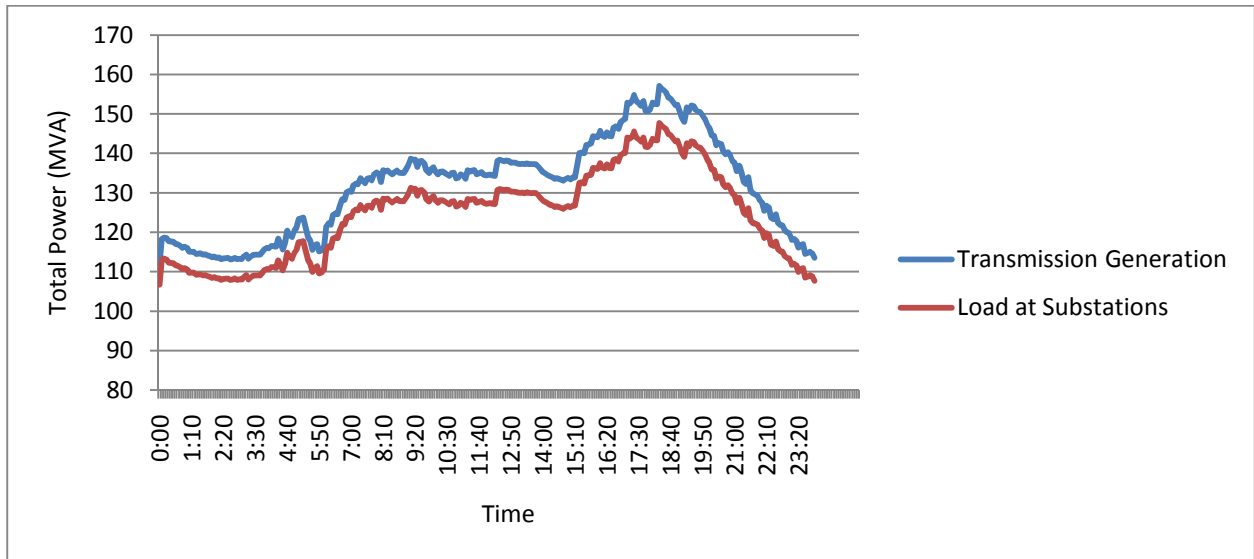
Figure 4.3: Generation at node 1 and the sum of load at substations for the base case

In addition to the output of the swing bus, automated capacitor and regulator controls are included on the distribution system to help regulate voltage. Distributed Energy Resources (DERs) were added at

various penetration levels and included energy storage and solar Photo-Voltaic (PV). The energy storage devices are intended to be generic models; they are not indicative of any particular technology and have a round-trip efficiency of approximately 80 percent. The storage devices are located at the substations and are locally controlled. The charge, discharge, or wait states are determined by monitoring the real power flowing into the feeder and providing or absorbing real power as needed. In the following use cases, the storage devices were sized to represent approximately 10% of the peak generation needed and were able to store 12 hours of useable energy. The solar panel and inverter combination are also intended to be generic models, converting solar insolation into real and reactive power, as indicated by the control method. The solar panels are distributed randomly throughout the feeder, attached at the 240 V household levels with a nameplate rating between 4 kW and 8 kW.

Climate data is also incorporated into the residential and solar panel models via Typical Meteorological Yearly (TMY2) Data from Phoenix,Arizona [6]. This is used to determine the solar insolation incident upon the solar panels, while solar input, air temperature, and humidity contributions are accounted for within the residential thermodynamic models. In the following cases, a very hot summer day in July was used to simulate extremely heavy loading conditions and high solar power production.

Four different cases were examined. The base case includes all of the features stated above, minus the solar panels and energy storage. Solar panels were then added at two different penetration levels: 5% and 12% of nameplate rating versus peak system power (40% and 100% physical penetration at residential levels). The solar panel and inverter combinations were controlled IAW IEEE 1547.2-2008, in which no direct voltage regulation is allowed. However, power factors were controlled to 1.0 and 0.85 lagging and the effects monitored. Finally, energy storage devices were added to mitigate the effects of the solar DER and the effects were studied.

4.2   Use Case 1: Reduction of System Losses

It is well understood that losses on a distribution system can be reduced if distributed generators (DGs) inject power into the system. A quantitative evaluation determining to what extent losses can be reduced on the distribution system and the effect on transmission system losses has not been fully conducted. This use case focuses on examining specific reductions in losses for various components at varying penetration levels of solar PV.

Losses at the sub-transmission level can be examined by observing the amount of power generated at the swing bus and comparing it to the total power delivered to all of the substations, in terms of both real and apparent power. In this system, the sub-transmission system consists of only overhead transmission lines. In Figure 4.4 and 4.5, the base case real and apparent power losses as a function of time are compared with the 5% and 12% solar cases when the solar generators are providing only real power. It can be seen that solar generation occurs between 6 a.m. and 7 p.m. and peaks at approximately 2 p.m. As expected, sub-transmission losses decrease during this time, while there is no effect when the sun is down. The amount can be quantified at high noon as an 18% reduction of real power losses and a 16% reduction of apparent power losses at 5% penetration. The effect is obviously even greater at 12% penetration with a reduction in real power losses of 33% and apparent power losses of 29%.
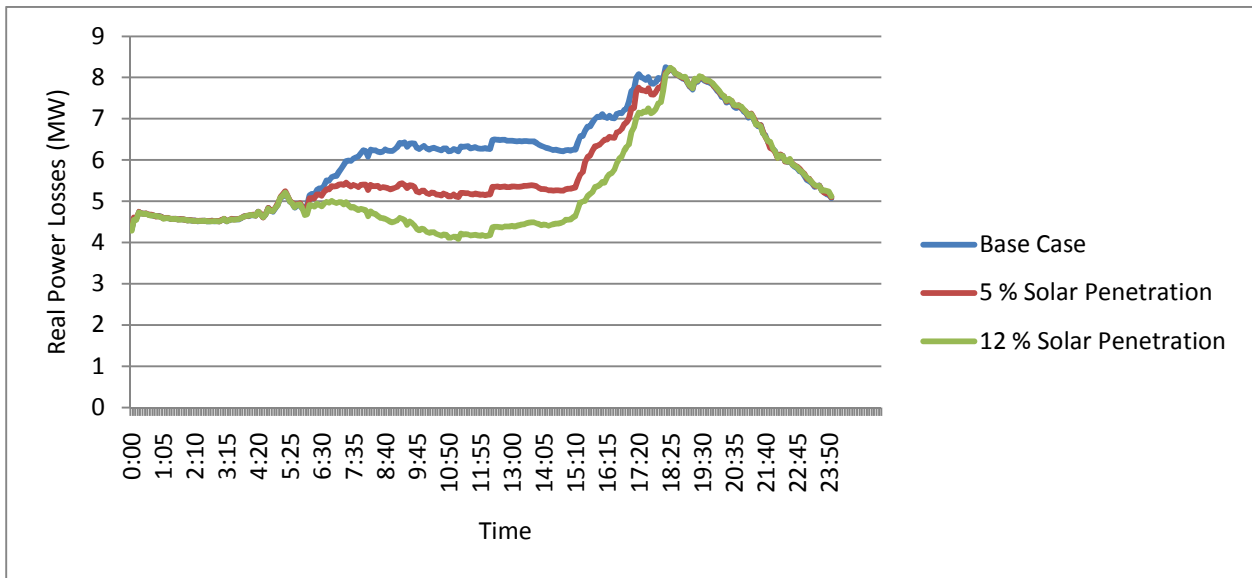
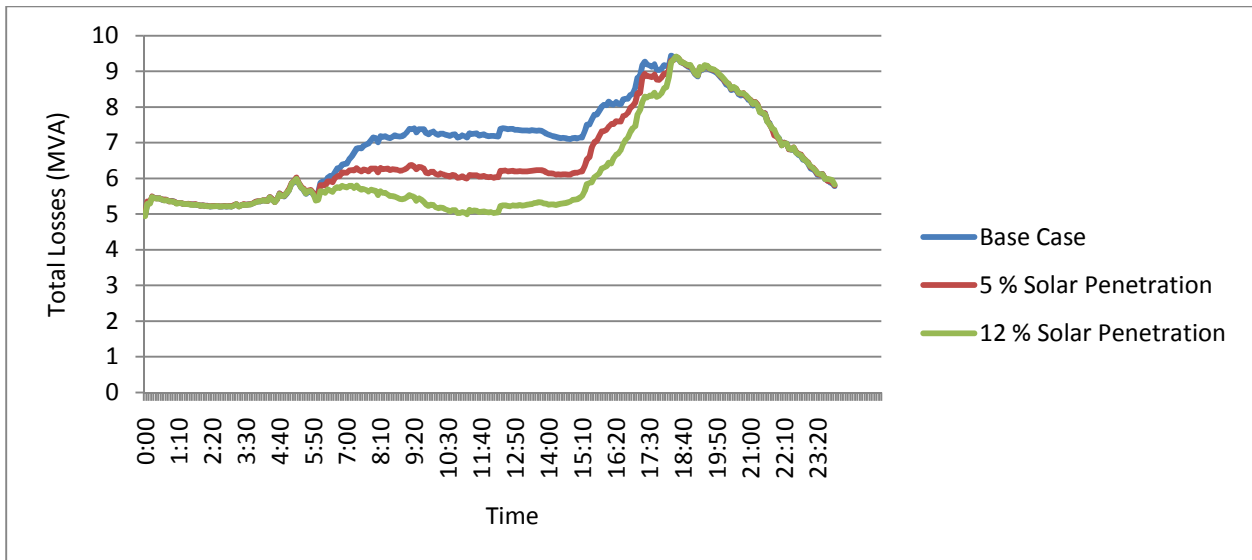**Figure 4.4: Real power losses on sub-transmission network**

Figure 4.5: Apparent power losses on sub-transmission network

Since solar power is not dispatchable, reduction in power loss does not always coincide with peak system losses. One potential solution is to combine energy storage devices and inverter control methodologies so that solar resources can be dispatched in a manner similar to traditional central

11

generating units. In Figures 4.6-4.9, the effects on sub-transmission losses can be seen at two different solar PV penetration levels, with and without reactive power support, and with and without energy storage. Figures 4.6 and 4.7 show the real power losses while Figures 4.8 and 4.9 show the apparent power losses.
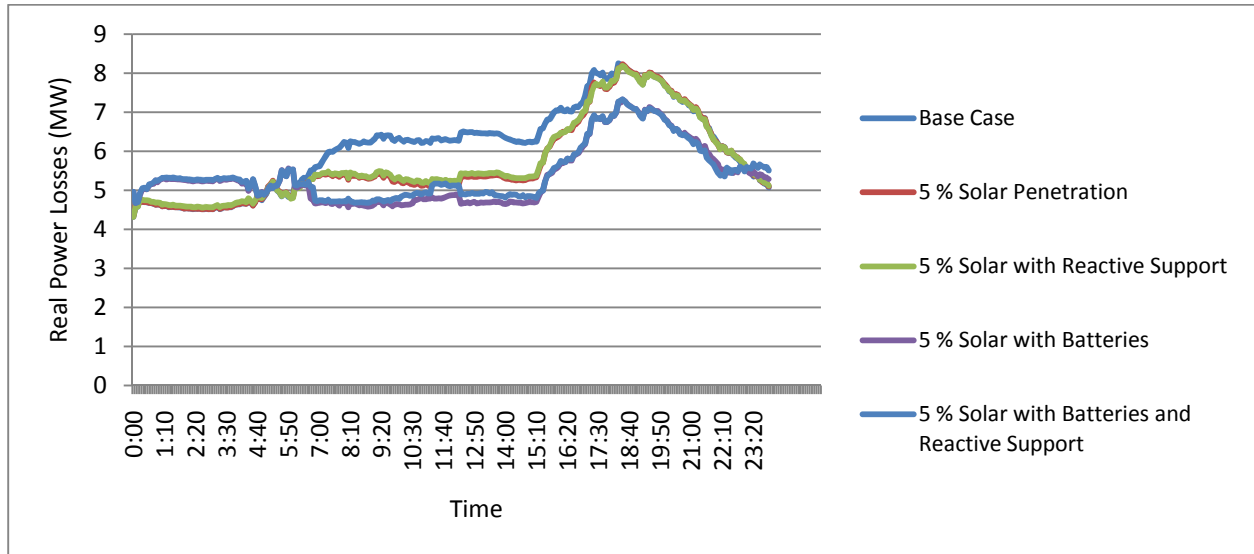
Figure 4.6: Real power losses at the sub-transmission level with reactive support and DER for 5% solar penetration
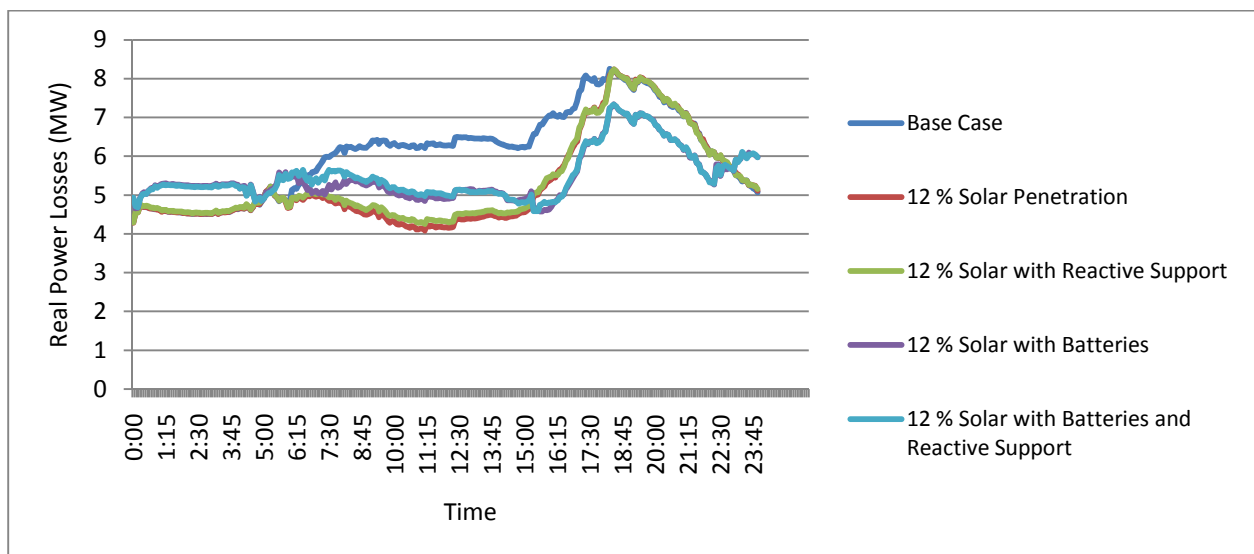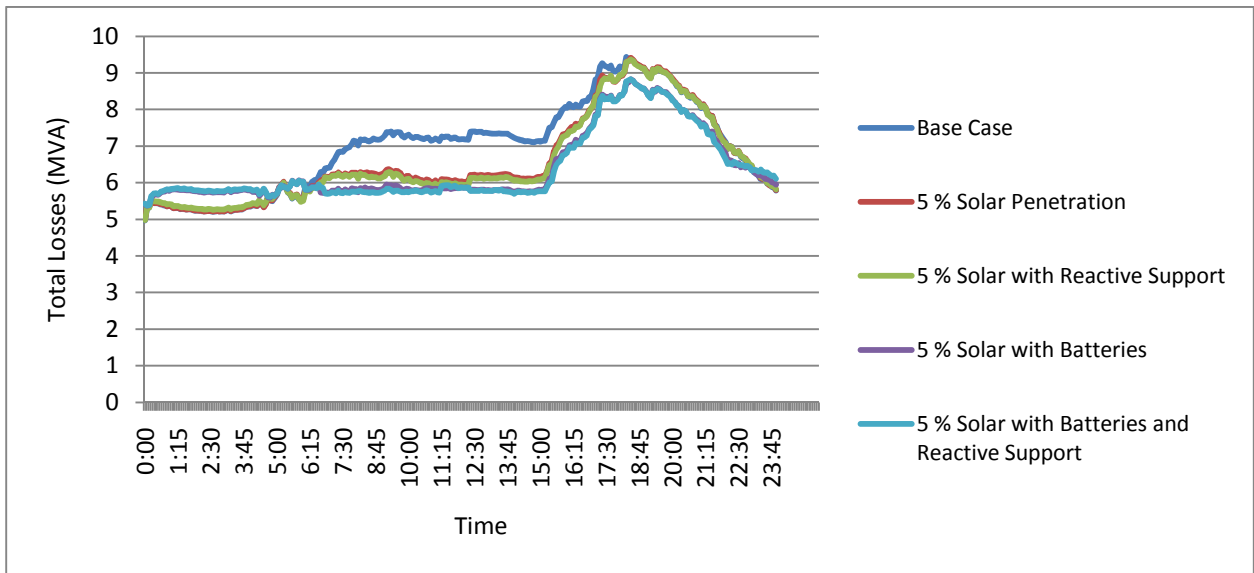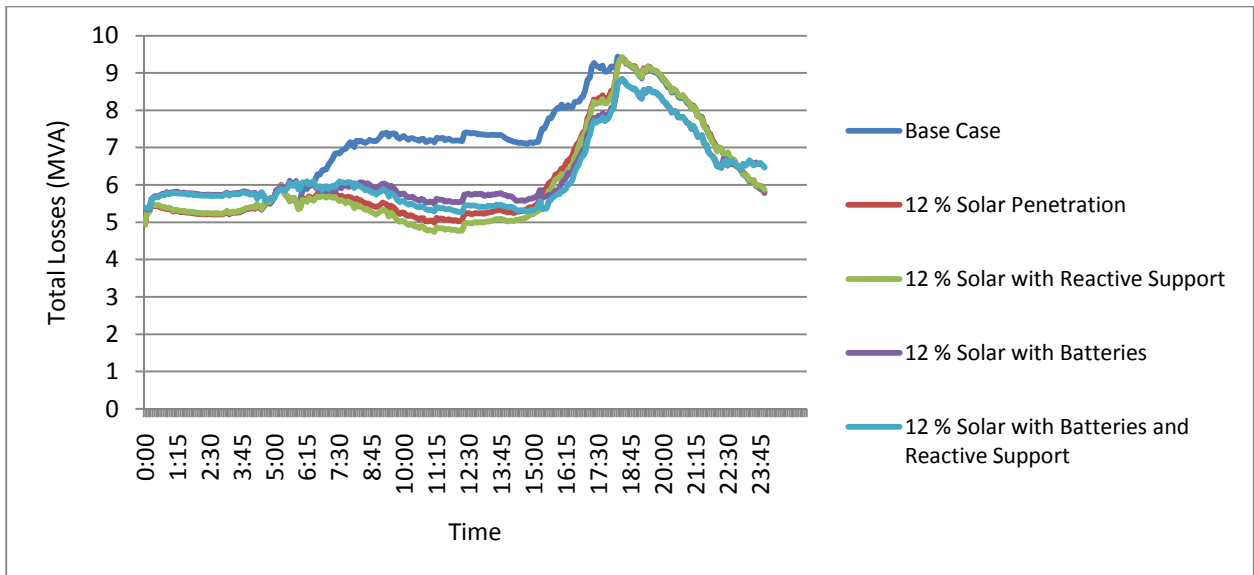

Figure 4.7: Real power losses at the sub-transmission level with reactive support and DER for 12% solar penetration

Figure 4.8: Apparent power losses at the sub-transmission level with reactive support and DER for 5% solar penetration


Figure 4.9: Apparent power losses at the sub-transmission level with reactive support and DER for 12% solar penetration

From Figures 4.6 through 4.9, a number of interesting items appear. For example, in all cases using energy storage devices, there is a significant reduction in losses during the discharge cycles at peak loading around 7 p.m. as compared to all other cases. However, when the energy storage devices are

charging during low power consumption periods, losses actually increase due to the increased load of the energy storage devices. During peak solar production at 12% penetration, transmission line losses increase slightly when battery support is included. Providing reactive power support at the solar panel has no significant effect on real power losses, but provides a slight reduction in apparent power losses over cases without reactive power support.

Other components within the system can also be evaluated in a similar manner. Figures 4.10 through 4.15 provide a similar analysis as performed on the transformers in the system, including the delta-grounded wye substation transformers and the residential center tap transformers. In this case, different outcomes can be seen as compared to the previous results. While solar penetration greatly decreases the amount of losses on the transformers, the effects of battery and reactive support behave differently. For example, the addition of storage devices at the substation does not reduce the losses on the residential center tap transformers. This is due to the fact that storage devices at the substation will not have a great effect on the power flow within the feeder itself, where most of the transformers are located. It will mostly have an effect on transmission level power flow. In addition, in Figures 4.13 and 4.15, it can be seen that reactive power support by the solar generators actually has a negative effect on power losses as reactive power is being pushed through the center tap transformers from the consumer side.
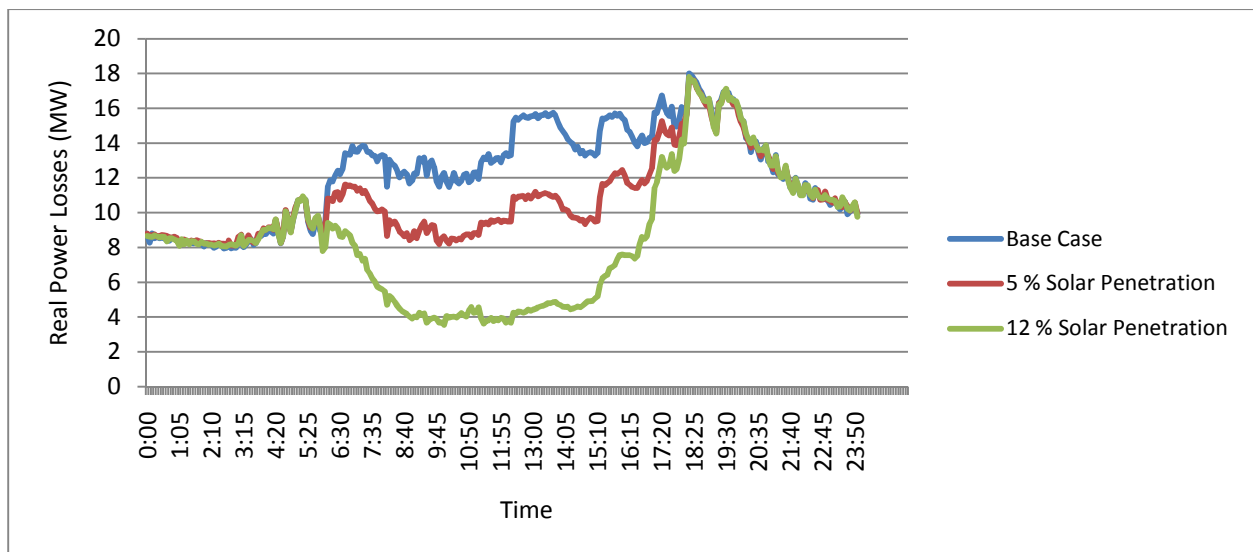
Figure 4.10: Real power losses of transformers on entire system at various DG levels
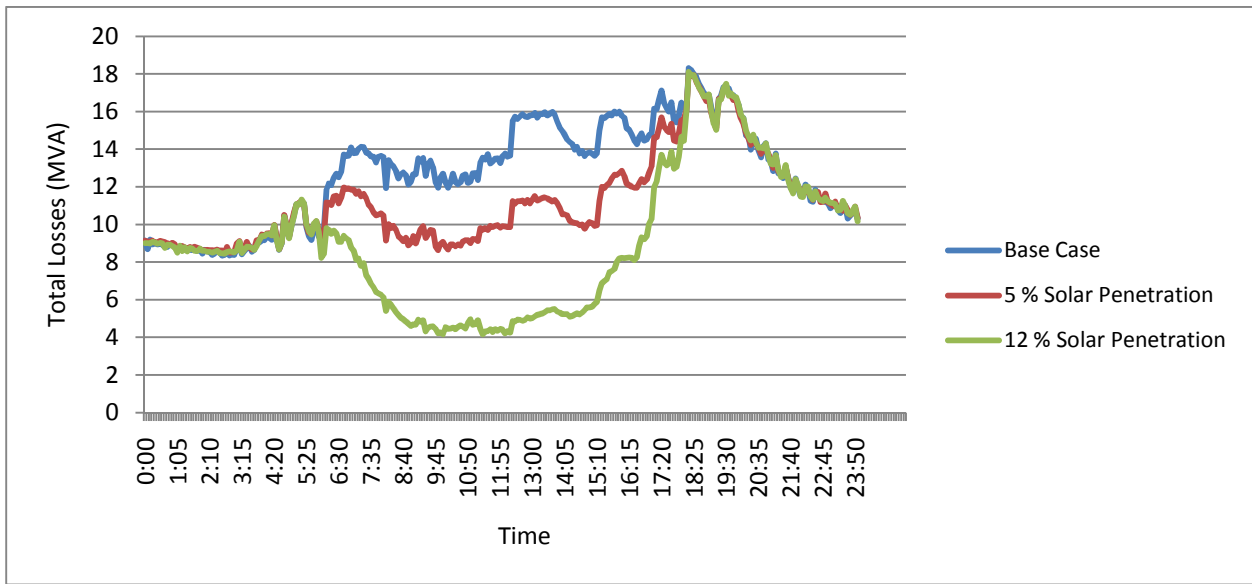
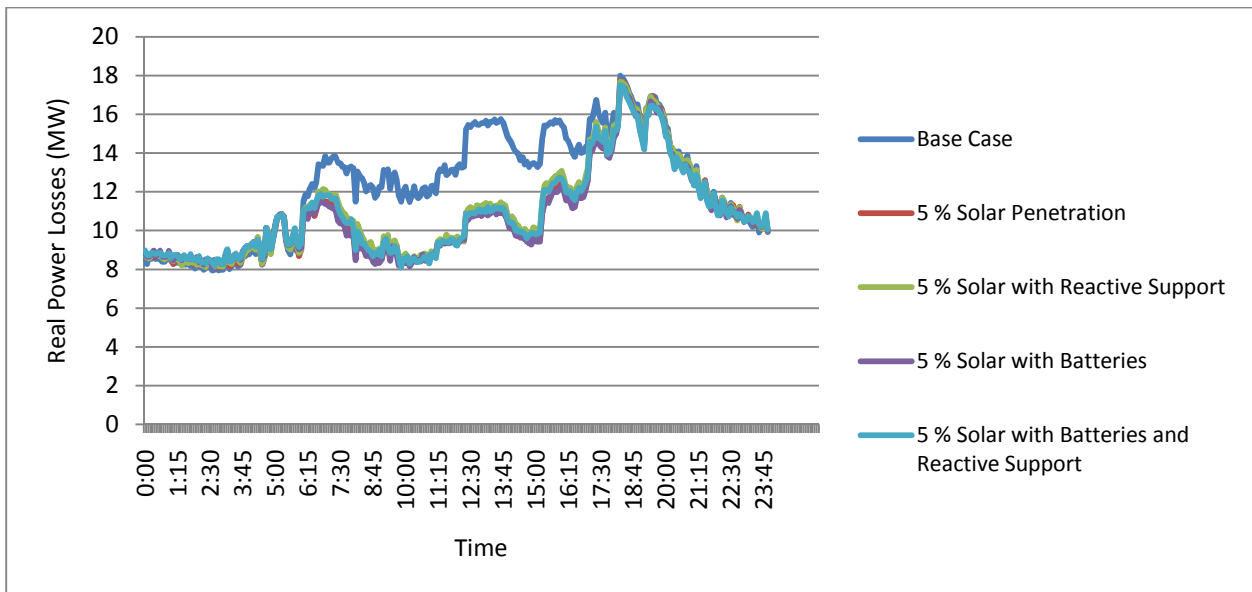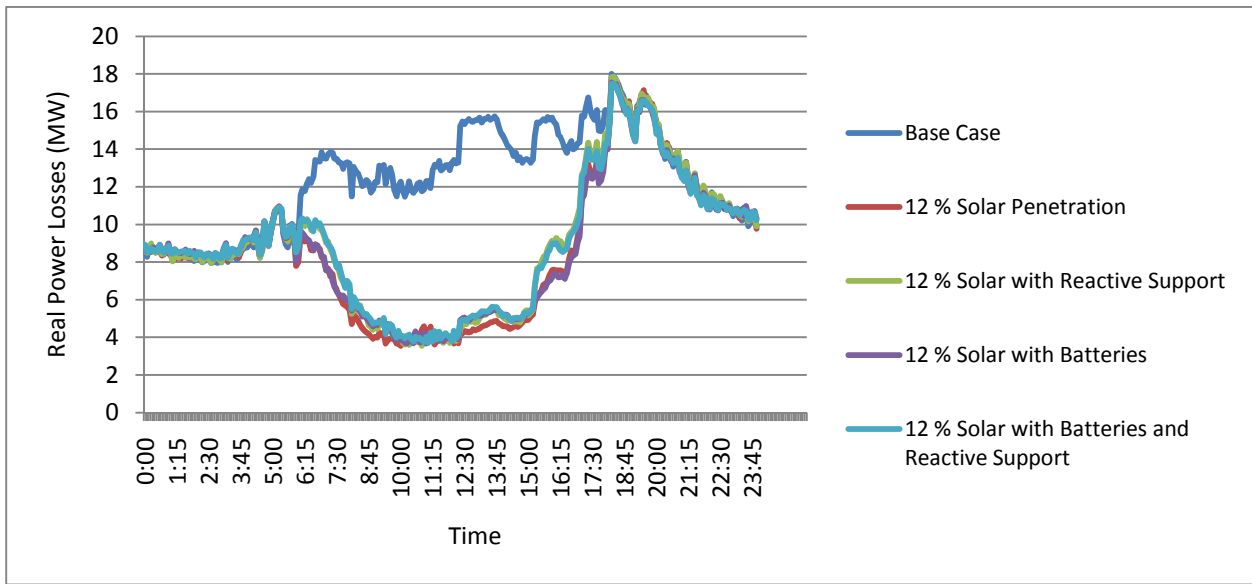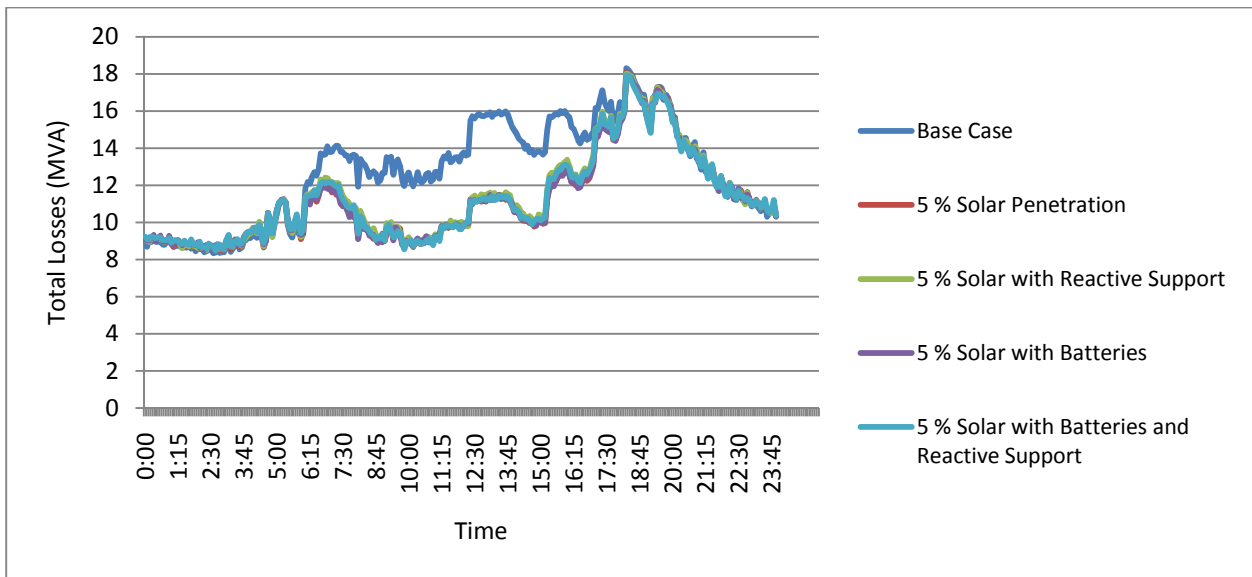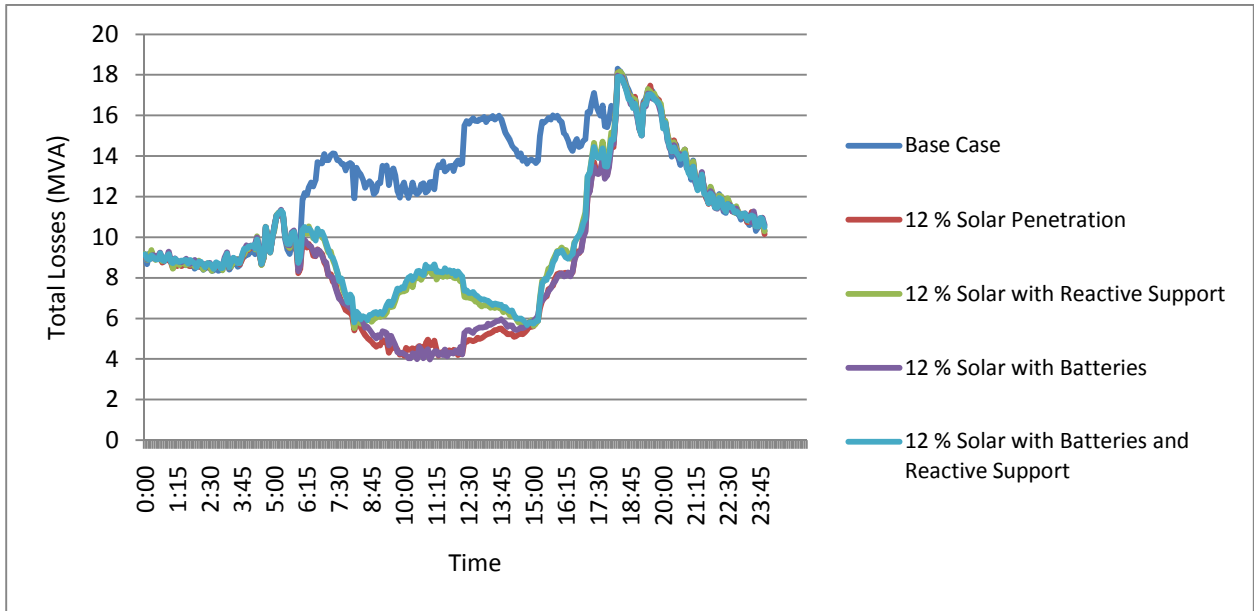**Figure 4.11: Apparent power losses of transformers on entire system at various DG levels**

Figure 4.12: Real power losses of transformers with reactive support and DR for 5% solar penetration

Figure 4.13: Real power losses of transformers with reactive support and DR for 12% solar penetration

Figure 4.14: Apparent power losses of transformers with reactive support and DR for 5% solar penetration

Figure 4.15: Apparent power losses of transformers with reactive support and DR for 12% solar penetration

While this is not a rigorous examination of all the effects of losses due to DER usage, it is an indication of what can be done with this software. Utility planners can determine what the needs of the system may be, target specific components, and determine the overall effects of implementing new technologies within the system, both at the transmission and distribution level.

4.3 Use Case 2: Reduction of Peak Demand

Distributed generation located on a distribution feeder can be used to schedule peak load reductions on distribution feeders if it is dispatchable. If the distributed generation is not dispatchable, then peak load reduction cannot be scheduled. As the level of renewable penetration increases, the ability to reduce the peak will increase. This reduction is due to both higher output capacity and a higher diversity, especially when energy storage devices are implemented. Reductions at peak periods have several significant impacts that can be examined. One impact is the effects of reduced loading on equipment, which has the potential to extend equipment life. This can be significant in highly loaded systems since the effect of temperature on lifetime is an exponent to the fourth power; as a result reductions in peak load can provide significant lifetime benefits. A second effect is the reduction in emissions that can be realized if the DG is a renewable resource or if it displaces high emission peaking units. The reduction in emissions due to peak demand reduction can be substantial because of the use of less efficient peaking units to meet the peak demand. Various operating strategies which conform to IEEE 1547 were examined, including the use of energy storage devices.

In this example, the total generation at the swing node will be observed. In Figure 4.16, total generation is compared for the base case versus 5% and 12% solar penetration with no controls or battery generation. It is apparent at what point solar power begins and ends to operate within the system. As

expected, peak production does not align with peak load, so there is no reduction of peak load. In fact, the 12% case shows a larger differential between low power consumption and peak power consumption. This is not ideal and it could result in the need to reduce central generation as the load decreases. Starting a central unit incurs high initial cost, and often higher emission rates as less efficient units are used as peaking support.
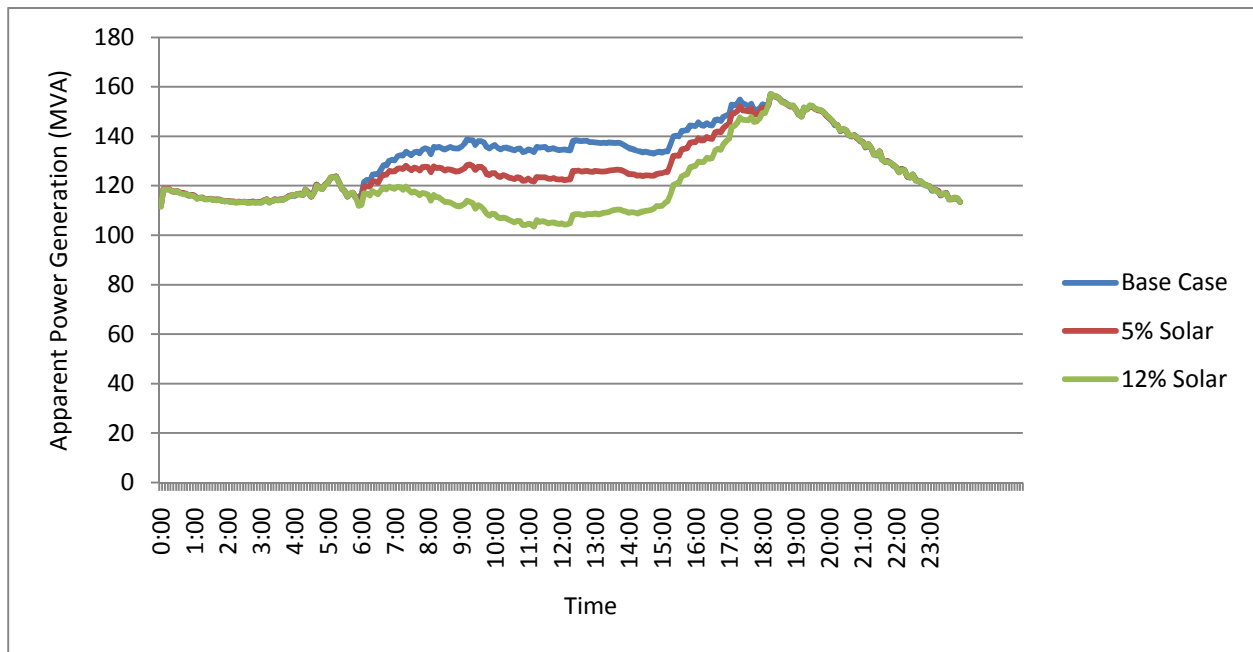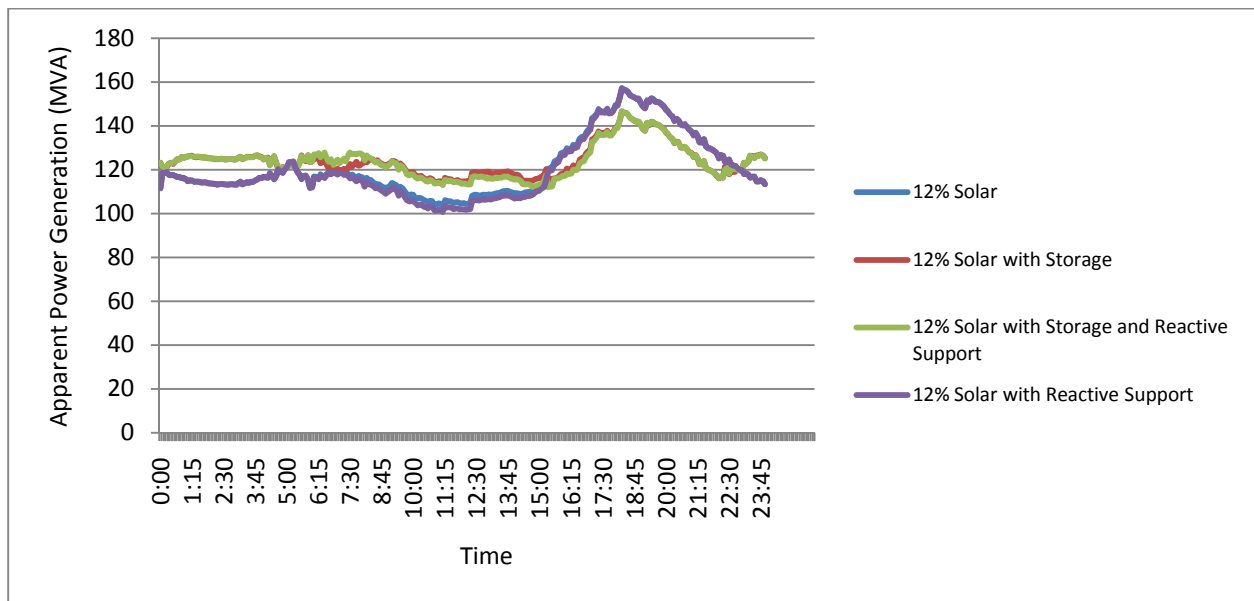

Figure 4.16: Total power generation at Node 1 with zero energy storage or reactive support

Figures 4.17 and 4.18 show the effects of applying the different control and storage strategies on the two levels of penetration, and the amount of sub-transmission level generation needed for each case. At both penetration levels, there is significant reduction of the peak load when energy storage is available. This amounts to a 7.8% reduction at 5% penetration and a 9.1% reduction at 12% penetration at 6 p.m. In addition, both penetration levels have a flatter load profile when energy storage is included, leading to fewer start-ups and shut downs of dispatchable generators. No real reduction is seen with the addition of reactive power assistance on any of the cases.
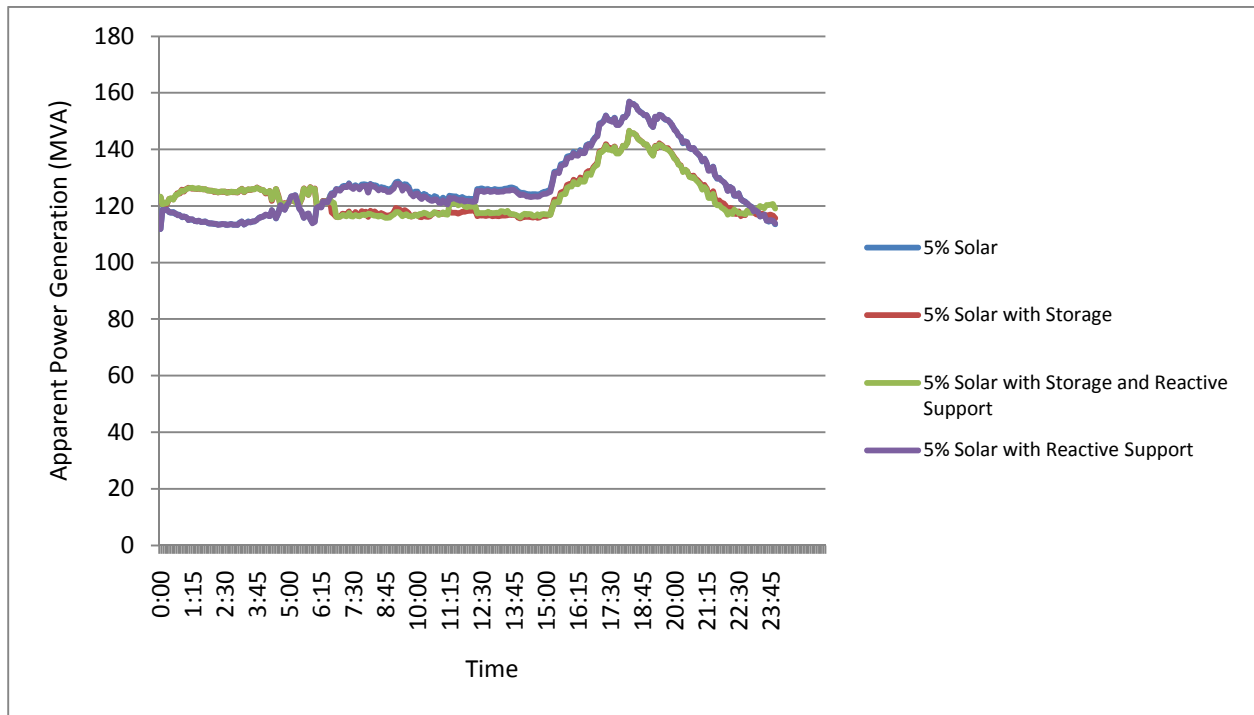
Figure 4.17: Total power generation at Node 1 with various methods with 5% solar penetration

Figure 4.18: Total power generation at Node 1 with various methods with 12% solar penetration

Since these simulations are performed over a period of time, the total energy consumption over the course of a day can also be compared. In Table 4.2 the energy consumption of each case is listed in order from the least amount of energy produced at the swing node to the most. As expected, all cases with energy storage are approximately the same, since energy storage only acts as a way to defer power production, and not reduce it completely. However, there is an 8.6% difference between the base case and 12% solar penetration with reactive support without storage, and a 3.5% reduction in energy generation between the base case and 5% solar penetration without storage. This reduction is composed of not only the effects of solar energy production, but also includes the reduction of losses associated with these configurations as seen in Use Case 1.

Table 4.2: Energy consumed over a 24 hour period via various cases

	Energy over 24 hours (MW-hrs)
12% Solar with Reactive Support	2890
12% Solar	2911
12% Solar with Storage and Reactive Support	2970
5% Solar with Storage	2970
5% Solar with Storage and Reactive Support	2973
12% Solar with Storage	2975
5% Solar with Reactive Support	3054
5% Solar	3061
Base Case	3161

## 4.4   Use Case 3: Reduction of Transmission Congestion

An issue of significant concern in transmission system operations is congestion management. Congestion is set to become an even more central issue as large installations of remotely located renewable resources are interconnected to the transmission systems, and as consumer load demand increases with the addition of Plug-In Hybrid Electric Vehicles and other high-demand user loads. One option to alleviate the expected congestion is to build additional transmission lines, which is an capital intensive and difficult process. Another option is to make use of local resources to alleviate transmission congestion. This use case will examine the feasibility of using distribution-level resources in order to reduce congestion on the transmission system. Operating strategies which conform to IEEE 1547 were examined.

The system modeled in Figure 4.19 was designed primarily to examine the interactions between the distribution and transmission system. Since it only has a single generator and the transmission conductors are oversized, it is not ideal for examining congestion. Despite this limitation, this use case will examine a simple case of congestion that will highlight how the analysis can be performed on larger systems.
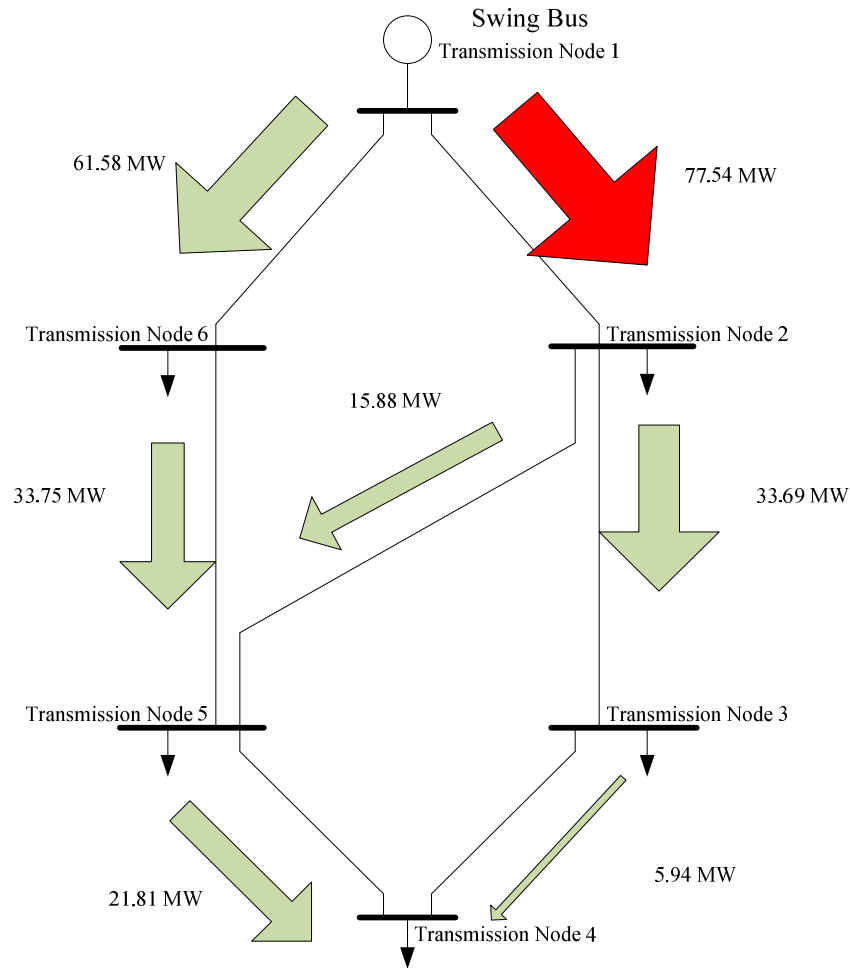
Figure 4.19: Congested system with no distributed resources

Figure 4.19 shows the peak power flows on the use case test system under the base case conditions; in the base case there are no distributed resources. The use case test system uses Hen-type conductors, which are operated at 138 kV, line to line. This cable type, operated at the indicated voltage, allows for a Total Transfer Capacity (TTC) of approximately 150 MW, which for this system is more than accurate. In order to develop the Transmission Congestion use case, it will be assumed that the TTC for the transmission lines is 75.00 MW with an Allowable Transfer Capacity (ATC) of 70 MW. Once again, this inaccuracy is introduced for the purposes of examining congestion management. As such, Figure 4.19 shows that there is a line violation between nodes 1 and 2. With this line congested, it means that additional generation, that is not supplied locally, cannot provide power. One option to address the congestion on the transmission system is to use resources on the distribution system. In this particular case, a combination of solar PV and energy storage is used to reduce the congestion, as shown in Figure 4.20.
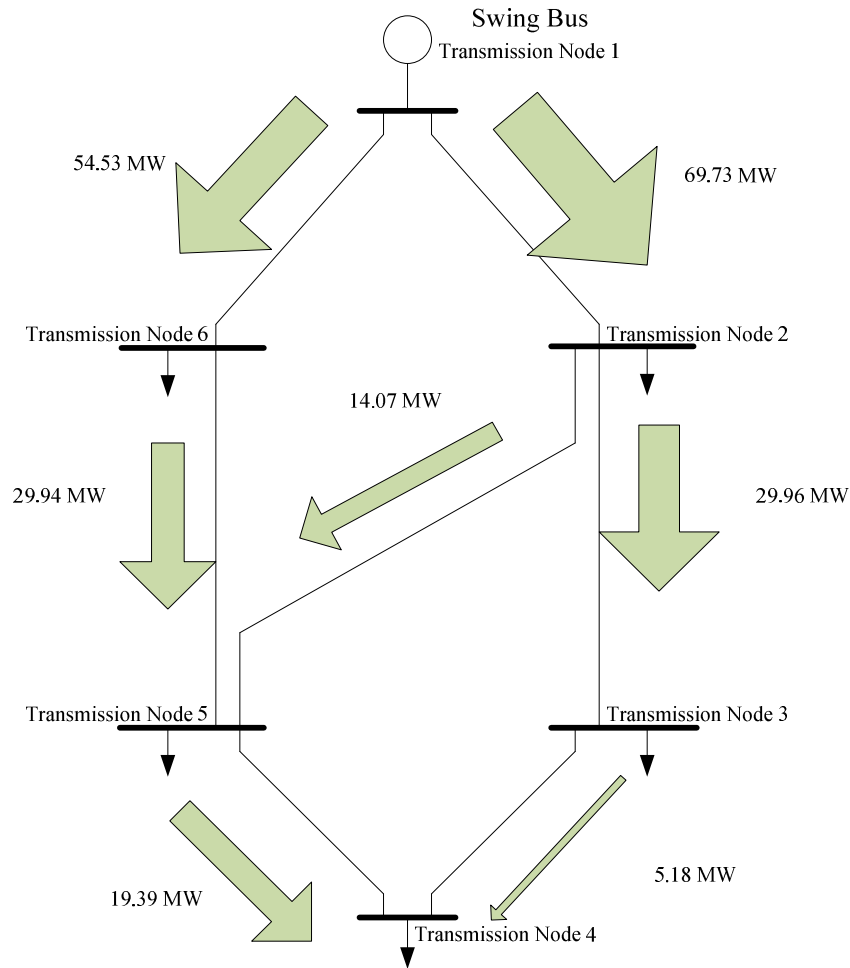
Figure 4.20: Uncongested system with distributed resources

4.5   Use Case 4: Coordination of Voltage Control and Power Factor Correction

Recently there has been increased interest in the area of voltage control and power factor correction for distribution system operations. This is partially due to the inefficiencies that have historically existed in distribution planning and operations. This use case examines methods of voltage control and power correction and their effects on their respective feeders, as well as the transmission system.

In this case, Conservation Voltage Reduction (CVR) is used on all of the cases without reactive support and energy, in addition to the other previously seen cases, and the effects upon losses and power factor correction are observed. In previous cases, voltage was monitored at a primary side node on the most heavily loaded section of the feeder. This voltage was then regulated to the nominal voltage (7200 V). Before applying CVR to the system, voltages were monitored throughout the system. It was found that the heavy loading on the system was already driving voltages near the lower ANSCII limit of 114 V on

heavily loaded areas, while rising to near the maximum of 126 V near lesser loaded areas [7]. However, as a hypothetical example, a voltage reduction of 100 V was applied at the 7200 V monitored node (an approximate 1.5 volt reduction on the 120 V consumer side), so that effects could be observed.

In Figures 4.21 through 4.24, the effects on generation power factor by the different control methods are examined. In Figure 4.21, the different solar penetration levels, with and without CVR, are shown with their respective effects on the power factor. As can be seen, the base case shows a fairly consistent power factor ranging between 0.915 and 0.930. However, as additional real-power-only solar generation is added to the system, there is a dramatic reduction in power factor. This leads to additional lost revenue within the generation plant itself. CVR has almost no effect on the power factor.
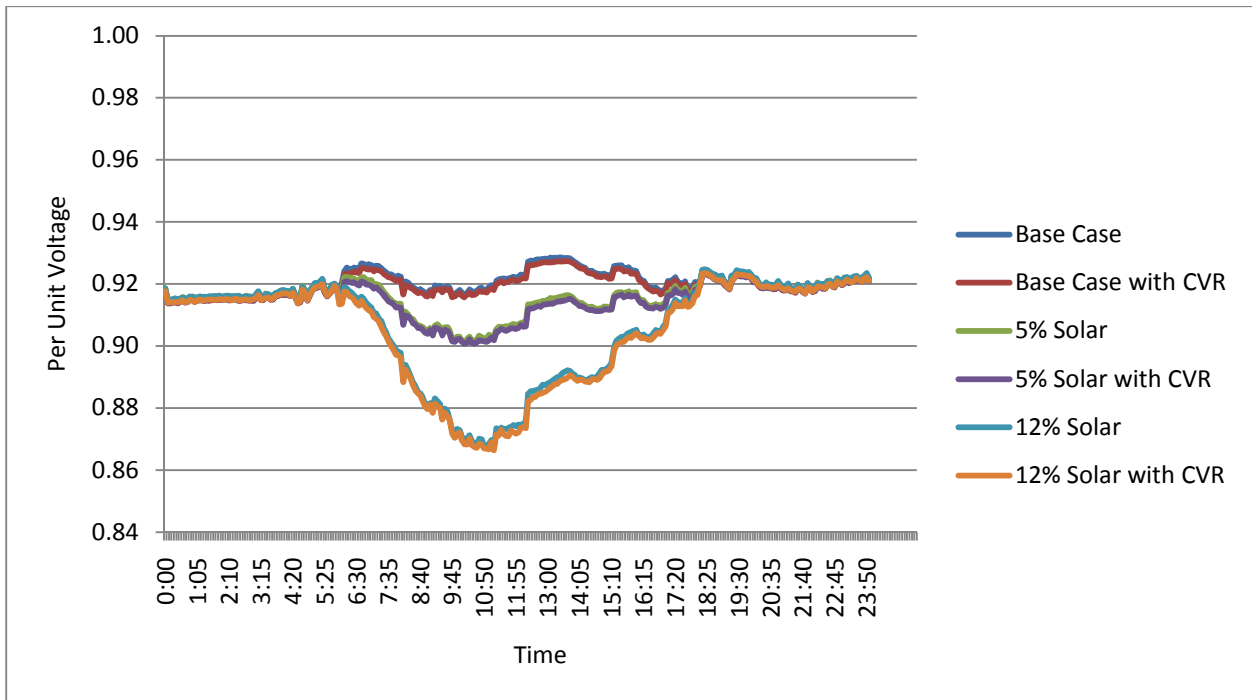
Figure 4.21: Effects of CVR and solar penetration on generation power factor

In Figures 4.22 through 4.24, energy storage and reactive support are added to the cases in Figure 4.21. The most noticeable effect at all three penetration levels is the effect of energy storage. The energy storage devices cause large swings in the power factor as they cycle between charge and discharge modes. This is due to the assumption that they would only absorb and provide real power; it is an indication that more appropriate control methods should be devised. A simple scheme could involve providing corrective power factors as opposed to purely real power. However, this would result in a reduction of energy available to flatten the load profiles. It would be up to the system planner to determine what an acceptable swing might be. However, it can be seen that when reactive support is provided by the solar panels, power factor is corrected considerably. At 5% penetration, the power factor ranges between 0.915 and 0.935, while at 12% penetration, it ranges between 0.915 and 0.945. On this system, a power factor

23

difference of 0.015 is equivalent to 2.5 MVAhr of generation that does not need to be provided and indicates a savings to the generator operator.
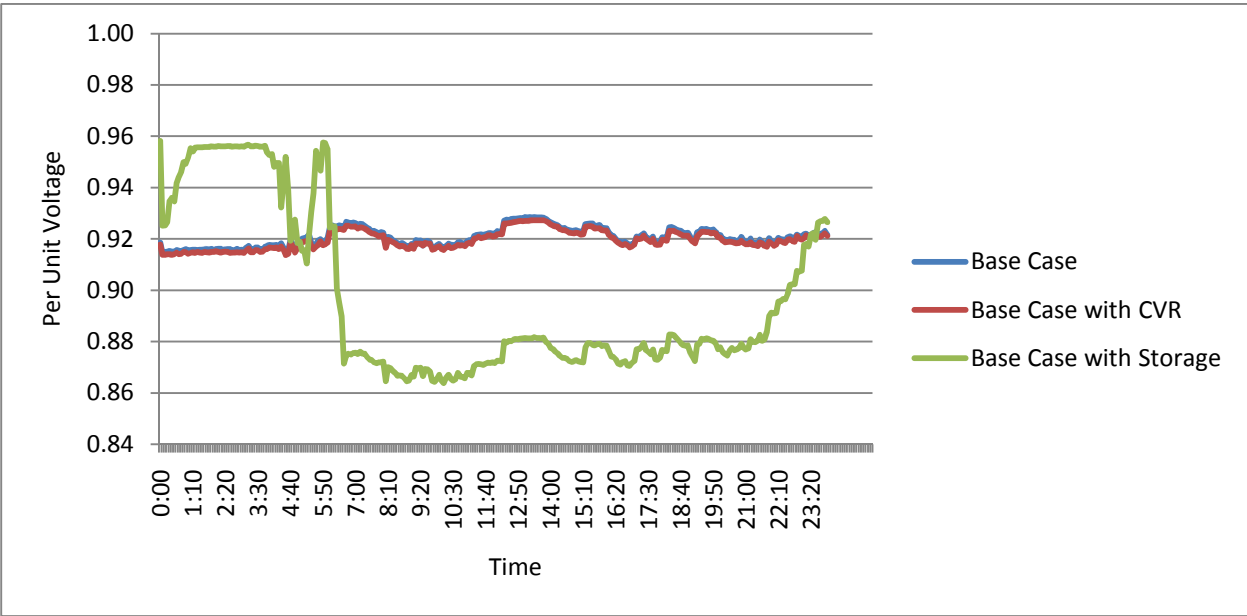

Figure 4.22: Effects of CVR and storage on generation power factor with 0% solar penetration
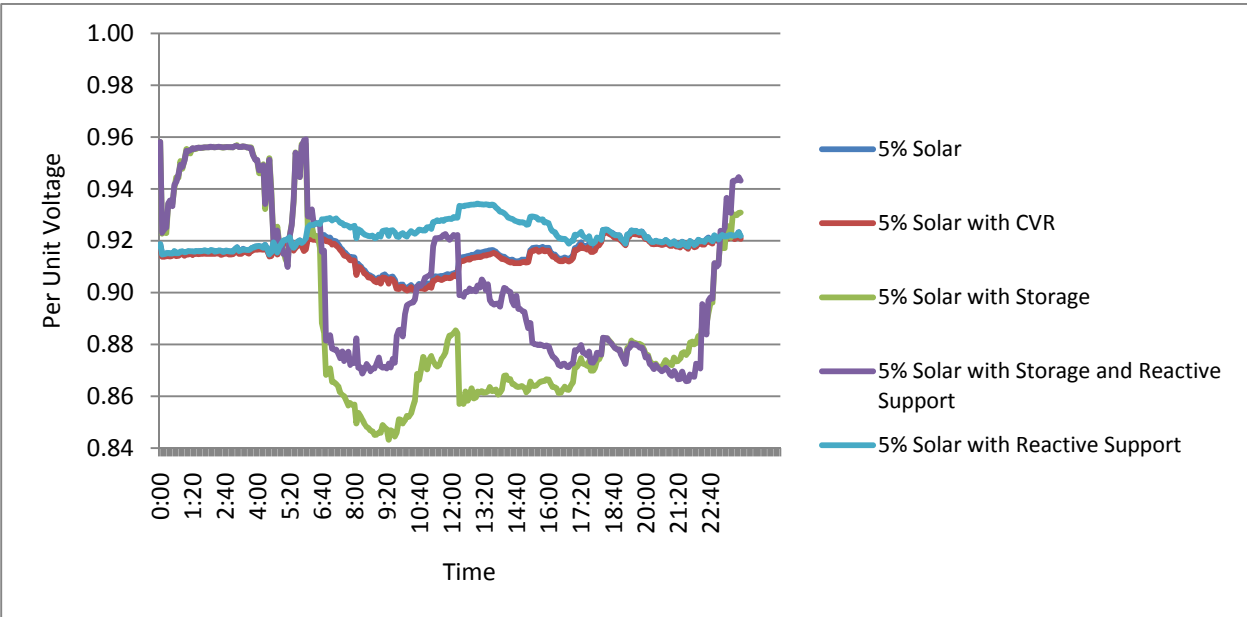

Figure 4.23: Effects of CVR and storage on generation power factor with 5% solar penetration
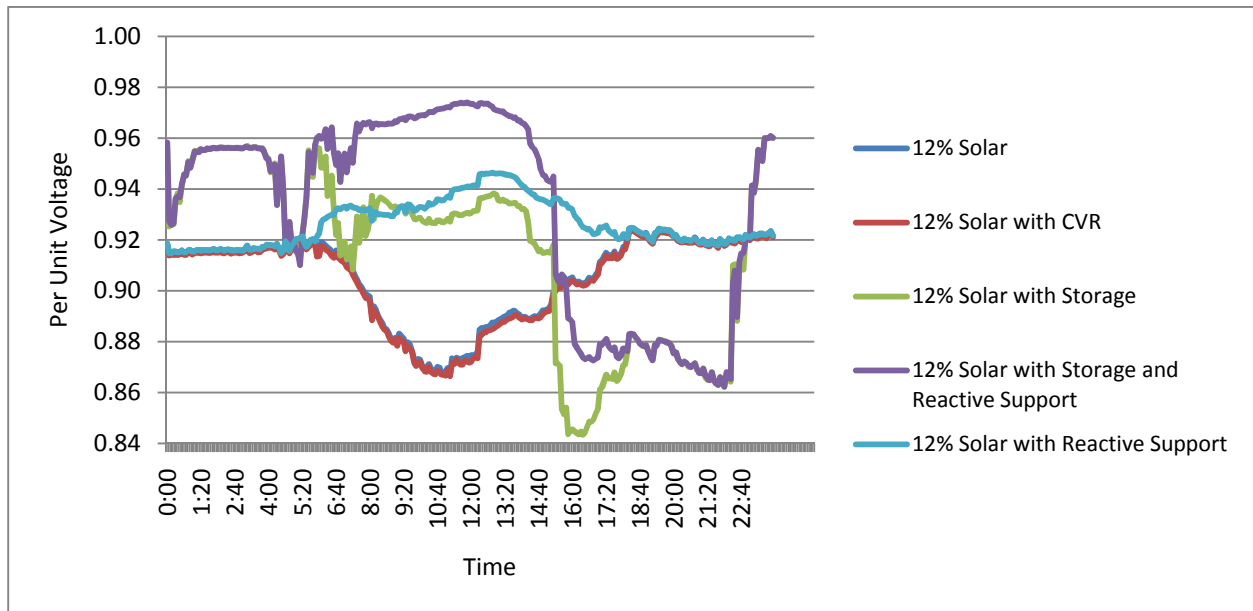
Figure 4.24: Effects of CVR and storage on generation power factor with 12% solar penetration

5. Closing Remarks

The work conducted by PNNL for the MGS in FY09 has significantly increased the capabilities of GridLAB-D. In particular the ability to examine the impacts of the emerging smart grid technologies has been enhanced. Integrated solvers that allow for the unified modeling of transmission and distributions with detailed end-use models will allow for the detailed analysis of a vast array of new technologies.

In addition to the new solvers that were developed in FY09, a set of use cases was developed to highlight the capabilities of the new solvers. Four specific use cases were developed and examined. These use cases were not meant to be a complete examination, but instead were meant to be templates for the type of integrated analysis that can now be performed. This form of integrated analysis is what will enable the analysis required to fully realize the potential of emerging smart grid technologies.

6. References

[1] http://sourceforge.net/apps/mediawiki/gridlab-d/index.php?title=Main_Page

[2] W. H. Kersting, "Distribution System Modeling and Analysis 2nd edition", Boca Raton: CRC Press, 2007.

[3] J. Grainger and W. Stevenson Jr., "Power System Analysis", McGraw-Hill, 1994.

[4] P. A. N. Garcia, J. L. R. Pereira, S. Carneiro Jr., V. M. Da Costa, and N. Martins, "Three-Phase Power Flow Calculations using the Current Injection Method", IEEE Transaction on Power Systems, Vol. 15, Issue 4, May 2000, pp. 508-514.

[5] K. P. Schneider, Y. Chen, D. Engle, and D. Chassin, "A Taxonomy of North American Radial Distribution Feeders", *IEEE PES General Meeting*, July 2009.

[6] National Renewable Energy Laboratory, "TMY2 User's Guide," *Renewable Resource Data Center*, available at http://rredc.nrel.gov/solar/pubs/tmy2/, Accessed September 30, 2009.

[7] ANCI C84.1-1995 (R2005).